Applied Energy 355 (2024) 122271

Contents lists available at ScienceDirect

Applied Energy

journal homepage: www.elsevier.com/locate/apenergy

Vanadium redox flow battery capacity loss mitigation strategy based on a comprehensive analysis of electrolyte imbalance effects

Thomas Puleston [*], Maria Serra, Ramon Costa-Castelló

Institut de Robòtica i Informàtica Industrial, CSIC-UPC, C/ Llorens i Artigas 4-6, 08028, Barcelona, Spain

ARTICLE INFO

Keywords:
Vanadium redox flow batteries
State of Charge
State of Health
Capacity loss mitigation
Electrolyte imbalance

ABSTRACT

Electrolyte imbalance is the main cause of capacity loss in vanadium redox flow batteries. It has been widely reported that imbalance caused by vanadium crossover can be readily recovered by remixing the electrolytes, while imbalance caused by a net oxidation of the electrolyte can only be reverted by means of more complex chemical or electrochemical methods. At the moment, however, the joint effect of both types of imbalances on the battery capacity is still not well understood. To overcome this limitation, generalised State of Charge and State of Health indicators that consider both types of imbalances are derived in this work. Subsequently, a thorough analysis on how the battery capacity depends on electrolyte imbalance is performed. As a result of this analysis, two specific outcomes are highlighted. Firstly, it is shown that standard electrolyte remixing may be counterproductive under certain imbalance conditions, further reducing the battery capacity instead of augmenting it. Secondly, it is demonstrated that most of the capacity loss caused by oxidation can be mitigated by inducing an optimal mass imbalance in the system. Consequently, a systematic procedure to track this optimum is proposed and validated through computer simulation.

1. Introduction

Nowadays, governments and international organisations are actively promoting the deployment of renewable energies to accelerate the transition towards a sustainable energy system. To properly manage the power generated by renewable energies, it is necessary to couple them with efficient and versatile energy storage systems [1]. Among them, all-vanadium redox flow batteries (VRFB) are now positioned as one of the most promising alternatives for large-scale stationary applications [2]. This is a consequence of the combination of a high round-trip efficiency (up to 85%), long lifespan (over 10000 cycles), simple and safe operation and their ability to reach a high depth-of-discharge [3]. A particular advantage of flow batteries is that, by storing the reactants in two independent reservoirs, the energy capacity becomes completely decoupled from the rated power, resulting in a flexible modular design with excellent scalability [4]. Besides, because of the utilisation of the same chemical element in both sides of the system, most of the cross-contamination problems that affect other types of redox flow batteries are eliminated.

In spite of VRFB remarkable merits, there are still some issues that need to be addressed in order to make them commercially competitive with other mature battery technologies, such as Li-ion. In particular, they are liable to undergo several side reactions that undermine their performance, diminishing their capacity and efficiency [5]. One of the most important consequences of these undesired phenomena is a condition known as electrolyte imbalance [6], i.e., a disequilibrium in the vanadium reactants concentrations.

Electrolyte imbalance is a critical issue in redox flow batteries. Most importantly, it leads to a capacity loss that is caused by the discrepancy in the number of moles of electron donor/acceptor species [7,8]. Moreover, when unnoticed, it may also give rise to additional negative consequences such as those associated to the electrolyte overcharging [9]. These include an acceleration of the gassing side reactions [10], a drop in the energy efficiency, and the corrosion of the electrodes and bipolar plates [11].

In this context, many works have been dedicated to study the causes of electrolyte imbalance in order to mitigate its progression and counteract its negative effects. It has been found that the best way to deal with the imbalance is strongly dependent on the causes that have originated it [12]. On the one hand, imbalance caused by a net transfer of vanadium moles from one side of the system to the other can be corrected in a simple manner by remixing the electrolytes content and evenly splitting the resulting solution into the two electrolyte tanks [8,13]. On the other hand, imbalance caused by side reactions that produce an oxidation or reduction of the vanadium ions can only be reverted by means of more complex and costly chemical or

---

[*] Corresponding author.
E-mail address: tpuleston@iri.upc.edu (T. Puleston).

https://doi.org/10.1016/j.apenergy.2023.122271
Received 7 February 2023; Received in revised form 29 September 2023; Accepted 4 November 2023

electrochemical methods [10,14], as will be explained in details in Section 2.3. At the moment, however, both types of imbalances have been addressed independently, not taking into consideration how their interaction affects the system's capacity.

To overcome this problem, in this work a new strategy that allows to substantially mitigate the negative effects of electrolyte imbalance is developed. The proposal is based on a thorough analysis of the combined effects of both types of imbalances on the battery capacity. In addition, in order to perform this analysis it is necessary to firstly redefine the expressions that allow to calculate the system's State of Charge (SoC) and State of Health (SoH) in terms of vanadium species concentrations, so that they can be valid for VRFB's that suffer from both types of imbalances. The formulation of these indexes is not a merely theoretical contribution, but also results of great interest to correctly plan the battery operation and for the development of control and estimation strategies.

The remainder of this work is structured as follows: Section 2 presents a general description of a VRFB system and the main side reactions that originate electrolyte imbalance, together with the specific background available in the literature to deal with this problem. In Section 3, generalised SoC and SoH indicators that consider the two main sources of electrolyte imbalance are derived. In Section 4, the effects of both types of imbalance on the battery's capacity are analytically decoupled and their interaction is discussed. Subsequently, a cost-effective strategy to maximise the battery's capacity is proposed. Section 5 presents comprehensive simulations to better understand the proposed strategy and assess its efficiency. Finally, Section 6 presents the conclusions of the work, collecting its main contributions and outlining some future research lines.

2. Electrolyte imbalance and existent solutions

A brief description of the fundamental operating principles of a VRFB is presented in this section. Afterwards, the main side reactions and undesired phenomena that affect VRFB are introduced and classified in terms of the type of electrolyte imbalance they produce. Finally, the existing approaches to mitigate and correct electrolyte imbalance and its associated capacity loss are discussed.

2.1. Vanadium redox flow batteries overview

In VRFB the energy is generated by the electron transfer reaction between vanadium ions with four different oxidation states [15,16]. Specifically, these are found in the electrolytes which consist of sulphuric acid solutions of vanadium salts. In the negative side of the system, the electrolyte (anloyte) contains the redox couple conformed by V^{2+} and V^{3+}. For its part, the positive electrolyte contains the oxides VO^{2+} and VO_2^+, respectively abbreviated as V^{4+} and V^{5+} because of the oxidation state of vanadium in those ions. The electrolytes are stored in two independent tanks, as illustrated in Fig. 1a. The system is completed with an electrochemical cell (or stack of cells) whose function is to generate the electric power; and an hydraulic system, responsible of connecting the tanks with the cell.

In normal operation, the electrolytes are continuously pumped from the tanks to the electrochemical stack, in order to guarantee a sufficient supply of the vanadium reactants required to produce the electric current. Inside the cells, the anolyte and the catholyte are kept separated by an exchange membrane that, ideally, allows only the passage of protons. The proton flux through the membrane allows to close the electric circuit internally and preserve the electrical neutrality of the solutions [17]. After leaving the cell, the electrolytes are returned to their respective tanks, thus closing the hydraulic circuit. In order to achieve a greater voltage and power, it is common practice to arrange groups of cells electrically in series to conform a stack.

VRFB are rechargeable so, when the battery is connected to an external power source, the reactions proceed in the inverse direction and the reactants are regenerated. The main electrochemical reactions that take place in the system, together with their standard potential, are the following:

At the negative electrode:

$$V^{2+} \underset{charge}{\overset{discharge}{\rightleftharpoons}} V^{3+} + e^- \qquad E_n^0 = -0.255\ \mathrm{V} \tag{1}$$

At the positive electrode:

$$VO_2^+ + 2H^+ + e^- \underset{charge}{\overset{discharge}{\rightleftharpoons}} VO^{2+} + H_2O \qquad E_p^0 = +1.004\ \mathrm{V} \tag{2}$$

2.2. Side reactions and electrolyte imbalance

Vanadium redox flow batteries are expected to be balanced. A VRFB is said to be balanced when both tanks contain the same liquid volume, and the concentrations of V^{5+} and V^{4+} in the positive electrolyte are equal to the concentrations of V^{2+} and V^{3+} in the negative electrolyte, respectively [14,18]. Ideally, when (1) and (2) are the only reactions occurring in the system, the VRFB will remain balanced provided that the electrolytes were originally balanced. However, as a consequence of several undesired phenomena, the electrolytes tend to become progressively imbalanced over extended charge–discharge cycling. This imbalance can be classified in stochiometric and faradaic imbalance [10]:

(a) Stoichiometric imbalance.

Stochiometric imbalance, also referred to as concentration imbalance [14], is associated to a difference in the total vanadium concentration between the catholyte and the anolyte. The main cause of stoichiometric imbalance is the undesired crossover of vanadium ions through the exchange membrane. After reaching the positive half-cell, V^{2+} and V^{3+} ions react rapidly with the V^{5+} ions present in the catholyte. Analogously, when V^{4+} and V^{5+} ions reach the negative half cell, they react with the V^{2+} ions of the anolyte. These reactions are typically known as self-discharge reactions and can be represented as follows [15]:

$$\text{In the negative half-cell:}\quad VO_2^+ + 2V^{2+} + 4H^+ \longrightarrow 3V^{3+} + 2H_2O \tag{3}$$

$$VO^{2+} + V^{2+} + 2H^+ \longrightarrow 2V^{3+} + H_2O \tag{4}$$

$$\text{In the positive half-cell:}\quad V^{2+} + 2VO_2^+ + 2H^+ \longrightarrow 3VO^{2+} + H_2O \tag{5}$$

$$V^{3+} + VO_2^+ \longrightarrow 2VO^{2+} \tag{6}$$

When the flux of V^{2+} and V^{3+} towards the positive half-cell is exactly the same as the flux of V^{5+} and V^{4+} towards the negative one, the crossover is said to be symmetric and its only effect is to produce electrolyte self-discharge [5]. However, crossover will be generally asymmetric, thus leading to a dilution of one of the electrolytes and an accumulation in the other.

A wide range of studies have been conducted to determine the causes of vanadium crossover. It has been found that it results from the combination of the mechanisms of diffusion, convection and migration. However, there is not a consensus on whether one of them prevail over the others. For instance, Tang et al. [19] found that crossover can be accurately modelled using a simple diffusion law. In contrast, Pugach et al. [20] showed via numerical simulation that, for certain membranes, convection is likely to be the dominant mechanism in a wide range of operating conditions. In general, it is now accepted that the relative contribution of each mechanism, as well as the magnitude and net direction of crossover, depends on the material of the exchange membrane as well as on the operating conditions [3]. In any case, it is clear that crossover cannot be completely eliminated and eventually would lead to imbalance in VRFB systems.

(b) Faradaic imbalance.

Faradaic imbalance is originated by those processes that lead to a net oxidation or reduction of the vanadium ions present in the electrolyte [10]. In normal operation, even in the presence of crossover

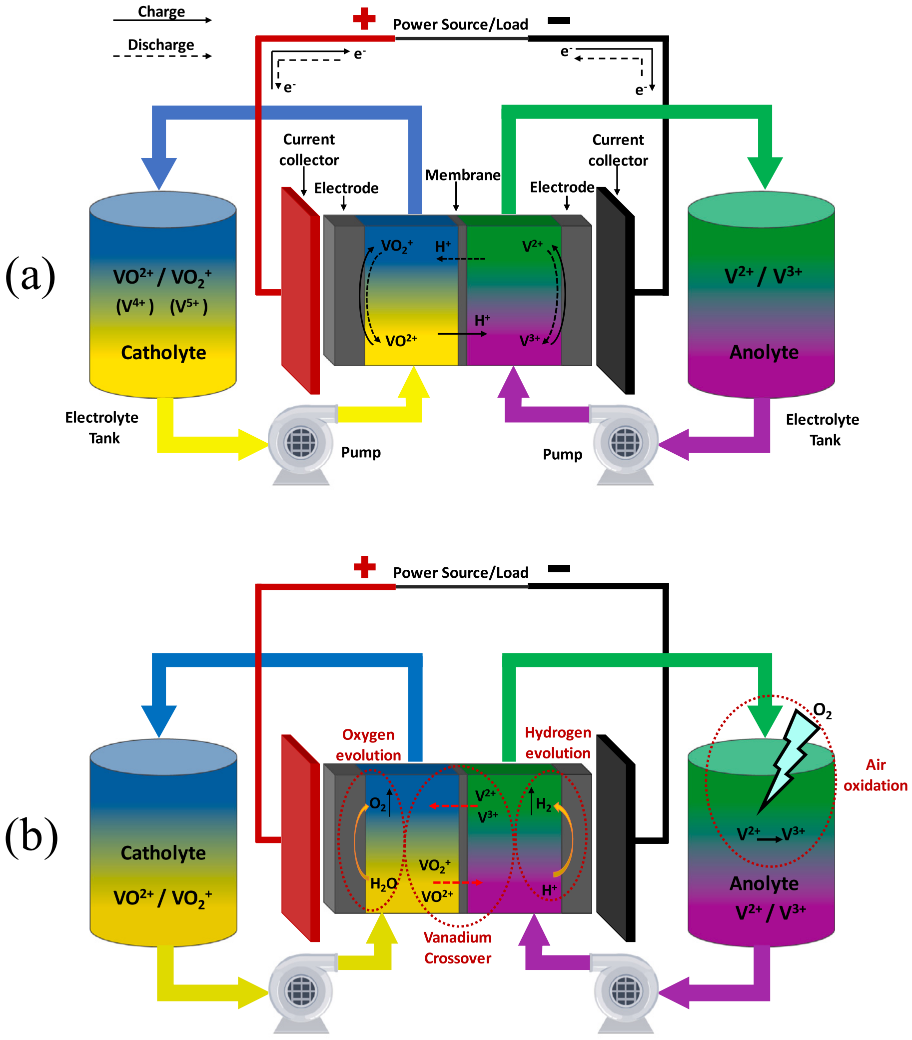

Fig. 1. Schematic of a VRFB with its main components, indicating (a) the ideal electrochemical reactions, and (b) its main undesired processes: vanadium crossover, gassing side reactions and oxidation with air.

and its associated reactions, the electrons are transferred only between vanadium species. Consequently, the average oxidation state of the system as a whole is not altered. However, there exists a second type of side reactions that produce an oxidation (or reduction) of vanadium species without a reduction (or oxidation) of another vanadium counterpart [21]. The main reactions included in this category are:

1. **Gassing side reactions.** These side reactions occur when species different to the vanadium ions, such as water and protons, start participating in the electron transfer reactions. The main side reaction included in this category is the so-called hydrogen evolution, that takes place at the negative electrode during charge operation [22,23]. Specifically, a fraction of the electrons that would normally be transferred to V^{3+} ions, are captured by the protons which get reduced to gaseous hydrogen (see Eq. (7)). Therefore, the reduction rate of V^{3+} at the negative electrode becomes slower than the oxidation of V^{4+} at the positive, hence causing electrolyte imbalance. In addition, other serious consequences associated to hydrogen evolution have been reported in the literature, such as the degradation of the carbon electrodes [24] and the bipolar plates [9]. The complementary gassing side reaction is the oxygen evolution at the positive electrode [25] (see Eq. (8)), which has similar effects as the hydrogen evolution although its occurrence is comparatively less frequent.

   $$\text{Hydrogen evolution:} \quad 2H^+ + 2e^- \longrightarrow H_2(g) \tag{7}$$

   $$\text{Oxygen evolution:} \quad 2H_2O \longrightarrow O_2(g) + 4H^+ + 4e^- \tag{8}$$

   It is worth mentioning that, from the thermodynamics point of view, H_2 evolution is favoured over the reduction of V^{3+} to V^{2+} at the negative electrode [10,23]. This is because the former has higher standard reduction potential ($E^0_{H^+/H_2} = 0$ V) than the latter ($E^0_{V^{3+}/V^{2+}} = -0.26$ V). It is only the sluggish kinetics of H_2 evolution on carbon electrodes what makes (7) occur at a much lower rate than (1). Therefore, despite being sometimes disregarded, hydrogen evolution remains always a possibility in VRFB [5].
2. **Air oxidation**. When the anolyte tank is not perfectly sealed, the oxygen present in the air tends to dissolve in the electrolyte and react with V^{2+} ions, oxidising them to V^{3+} [26]:

   $$\text{Air oxidation:} \quad O_2 + 4V^{2+} + 4H^+ \longrightarrow 4V^{3+} + 4H_2O \tag{9}$$

   In order to prevent air oxidation, it is crucial to keep the negative electrolyte tank isolated from the atmosphere. Besides, this phenomenon can also be minimised by periodically purging the electrolyte with an inert gas, such as nitrogen [27]. However, although these measures contribute to substantially reduce the oxidation rate, it is difficult to achieve a complete protection [10].

Fig. 1b illustrates the main side reactions that have been presented in this section. These constitute the most common causes of electrolyte imbalance given their continuous and often unavoidable nature. Nonetheless, it should be remarked that there exist additional processes or events that may lead to electrolyte imbalance. For instance, a damaging event that produces an electrolyte leakage in one of the tanks would result in a VRFB with both faradaic and stoichiometric imbalances.

2.3. Background on electrolyte imbalance mitigation and recovery

The aforementioned side reactions actuate even when the battery is correctly operated, unavoidably leading to electrolyte imbalance after extended operation. Consequently, many efforts are being done to develop strategies to mitigate and correct this imbalance.

Stoichiometric imbalance can be reverted in a relatively easy way, with several methods being described in the literature. By far, the most popular of them is the electrolytes remix [10,28]. This strategy consists of mixing the contents of both electrolytes and, subsequently, evenly redistributing the resulting mixture into the two tanks. When both electrolytes are put in contact, reactions (3)–(6) take place, producing a solution that contains V^{3+} and V^{4+} in proportion 1:1, often referred to as $V^{3.5+}$. After the remix, the volume and vanadium concentration in each tank become perfectly equalised [10]. To avoid the interruption of the battery operation as well as its full discharge, it has also been proposed to perform a partial remix [8], i.e., transferring small aliquots of electrolyte from one tank to the other, just to compensate the effects of crossover.

Other authors have focused on strategies to mitigate the progression of stoichiometric imbalance rather than correcting it. For instance, Wang et al. [29] introduced a very simple method that consisted in a reflow from the positive tank to the negative, to counteract the volume change that spontaneously tends to increase the volume of the positive electrolyte at the expense of the negative. In the same line, Schafner et al. [30] applied a very similar method and concluded, by computer simulation, that despite the capacity loss is minimised with an overflow strategy, an electrolyte remix is eventually necessary to completely correct the stoichiometric imbalances. Bhattarai et al. [31] experimentally found that placing an hydraulic shunt, namely a long narrow tube that connects both tanks at their bottom, permits to minimise the capacity loss. However, the working principle of this method is not explained in detail, and it is possibly just another way to prevent an electrolyte volume change. A different approach to mitigate the capacity fade is to periodically add fresh electrolyte to the negative tank [32,33]. However, this implies consuming more electrolyte and, furthermore, it is not clear why it is convenient to add it in stages instead of just increasing the initial volume. Shin et al. [34] proposed, and experimentally validated, utilising a higher concentration of sulphuric acid in the anolyte than in the catholyte to minimise the volume change and the electrolyte imbalance. Finally, Lu et al. [35] found that crossover and its associated capacity loss can be minimised by utilising a higher vanadium concentration in the positive electrolyte, in order to compensate the difference in vanadium species diffusivities. In addition, they demonstrated that crossover can also be mitigated by setting an asymmetric operating pressure in both half cells to induce a convective flux in a direction opposed to diffusion.

Faradaic imbalance, on the other hand, is considerably less easy to deal with. The oxidation (or reduction) processes previously discussed produce a shift in the average oxidation state of the whole system [14,36]. Therefore, if remixed, the ratio between V^{3+} and V^{4+} would not be 1:1. In other words, the average oxidation state will be higher than +3.5 (oxidative imbalance) or lower than +3.5 (reductive imbalance). Consequently, the capacity of the battery would remain diminished even after remixed. Accordingly, to restore the capacity of a faradaic imbalanced VRFB, it is necessary to resort to more complex chemical or electrochemical methods.

Roznyatovskaya [37] introduced a method that allows to fully recover the capacity of the battery by charging the imbalanced electrolytes, and subsequently replacing a part of the catholyte by fresh $V^{3.5+}$ electrolyte. Although simple and effective, that method requires of an external supply of electrolyte to compensate the removed part, somewhat limiting its applicability. In [21], an alternative hydraulic circuit that connects both tanks to each other is included in the system. Then, when the VRFB is operated in “recovery mode” this alternative path is enabled, resulting in the full mixing of the electrolytes. Afterwards, the desired average valence of +3.5 system is restored by means of an electrochemical cell. This cell utilises an auxiliary electrolyte to reduce the vanadium, and is equipped with an optical sensor to detect the correct endpoint of the electrolysis. More recently, Poli et al. [14] proposed to couple the system with an electrochemical cell that is placed in parallel to the main hydraulic circuit. This method outperforms the former, in the sense that it is not needed to interrupt the operation to recover the electrolyte and, furthermore, the electrolysis does not require an auxiliary reducing agent, but the anodic reaction is the oxygen evolution from the water contained in the electrolyte. Finally, it has also been proposed the addition of external reducing/oxidising agents to the system, such as methanol or oxalic acid [6].

To the best of our knowledge, the only work that has considered the joint effects of faradaic and stoichiometric imbalances on the battery capacity is that recently published by Wang and collaborators [38]. In that work, it is proposed to utilise an electrolyte with an elevated average valence, to mitigate the effects of stoichiometric imbalance when the crossover goes towards the positive electrolyte. Although very interesting results are shown in that work, the analysis is mostly restricted to that specific case and, furthermore, does not consider the possibility of a spontaneous progression of the faradaic imbalance.

The analysis carried out in this section can be summarised with two final remarks. In first place, it has been shown that stoichiometric imbalance can be corrected in a much easier way than faradaic imbalance, which requires of additional equipment or reactants. Secondly, it has been found that VRFB are prone to suffer from both stoichiometric and faradaic imbalance after extended operation. However, as anticipated in Section 1, the interaction between these two types of imbalance has not been analysed and thus, these are normally addressed independently. In this work, such interaction is considered, allowing to better understand the relation between electrolyte imbalance and the battery capacity. Based on that analysis, the design of a new approach to maximise the capacity of an imbalanced VRFB will be explored.

3. Generalised indicators formulation

In this section, new indexes will be defined to describe the battery available charge, namely, the State of Charge; and the maximum charge capacity, namely, the State of Health. Specifically, generalised expressions in terms of the vanadium species number of moles will be derived and explained through illustrative examples. These proposed expressions should be capable to deal with the two types of electrolyte imbalance described in Section 2. For clarification regarding the meaning of the variables that appear in this section, please refer to the nomenclature summary included at the end of this paper.

3.1. State of charge

The SoC is defined as the ratio between the level of charge stored in the battery (Q) at a specific point in time and the total battery capacity (Q_M) [39], as expressed in Eq. (10). Then, the objective of this subsection is to derive a mol-based expression for the SoC that is compatible with (10), even in the presence of electrolyte imbalance.

$$\mathrm{SoC} = \frac{Q}{Q_M} \tag{10}$$

The electrical charge in a VRFB system is directly related to the amount of vanadium "charged species" (V^{2+} and V^{5+}) present in the electrolyte. Consequently, assuming that the battery is balanced, the resulting expression for the SoC in terms of the vanadium number of moles is:

$$\mathrm{SoC} = \frac{M_2}{M_2 + M_3} = \frac{M_5}{M_4 + M_5} \tag{11}$$

where M_i is the number of moles in the battery of the vanadium species with oxidation state $+i$.

Eq. (11) is very popular in the literature [18,39] and has a clear physical interpretation. The numerator represents the electric charge that is currently stored in the system, which is given by the number of moles of the system charged species at present time. In turn, the denominator is the total electric charge the system can deliver from fully charged, i.e., the total battery capacity. Accordingly, it is given by the sum of the charged species and the discharged ones.

Before proceeding with the development of the new generalised expressions, it is important to state three clarifying remarks:

1. Strictly speaking, it is necessary to multiply the number of moles by the Faraday constant ($F = 96485$ C/mol) to obtain the electric charge of the battery. However, to ease the reading and avoid unnecessary reiterations, in the remainder of this paper, the battery's charge will be normally expressed in terms of moles.
2. In the literature, Eq. (11) is more commonly presented in terms of the vanadium species concentrations (c_i) rather than the number of moles. In this paper, however, the formulations are based on the number of moles, since this allows to consider also volumetric imbalances in the system, thus being more general. Evidently, when both electrolytes have the same volume, the formulations in terms of the number of moles become completely equivalent to those based on concentrations.
3. In Eq. (11) it is assumed that the battery is fully discharged ($\mathrm{SoC} = 0$) when the concentration of reactants is equal to 0. That convention is preserved in this paper: SoC = 0 corresponds to a situation where, at least one side, charged species concentration (V^{2+} and V^{5+}) is equal to 0, whereas SoC = 1 corresponds to the situation where, at least in one side, discharged species concentration (V^{3+} and V^{4+}) is 0. In practice, the SoC operating range will be normally narrower, rarely falling below 10% in discharge or surpassing 90% in charge.

When the VRFB suffers from electrolyte imbalance, Eq. (11) is no longer valid, and it is usual to define a SoC for each side of the system:

In the anolyte: $$\mathrm{SoC}_n = \frac{M_2}{M_2 + M_3} \tag{12}$$

In the catholyte: $$\mathrm{SoC}_p = \frac{M_5}{M_4 + M_5} \tag{13}$$

Despite having defined two independent SoC for each of the electrolytes, the overall VRFB SoC is still an important variable, as it indicates the percentage of the charge that the battery can effectively provide, in relation to its total capacity. Then, some authors [40] propose to directly define it in terms of the electrolyte with the lowest SoC: $\mathrm{SoC} = \min\{\mathrm{SoC}_n, \mathrm{SoC}_p\}$.

However, this SoC interpretation contradicts the original definition expressed in Eq. (10) because it does not take into account the fact that, when imbalanced, a part of the total vanadium species present in both sides of the VRFB is no longer able to react with their counterparts. For example, let us consider a VRFB that contains 10 moles of vanadium in each electrolyte but, at a certain instant, $\mathrm{SoC}_n = 40\%$ and $\mathrm{SoC}_p = 60\%$, as depicted in Fig. 2. Then, the resulting SoC of the battery applying the previous formula would be 40%. However, if that VRFB is subsequently charged, the maximum amount of V^{2+} would be 8 *mol*, because of the absence of electron-donor species (V^{4+}) in the positive side, as can be appreciated in Fig. 2. Then, the SoC computed with the traditional formula would have an upper bound of 80% instead of the 100% established in (10).

Therefore, the example presented in Fig. 2 can be used to illustrate the derivation of an expression of the SoC consistent with (10). If the battery is imbalanced, the charge it can deliver will be given by the charged species that is in least amount. This is, the numerator in the generalised SoC expression will be the minimum between M_2 and M_5. In the example, the charge delivered by the battery from the present state (Fig. 2i) to fully discharged (Fig. 2iii) is precisely that corresponding to the 4 moles of V^{2+} present in Fig. 2i. As for the maximum charge the battery can provide from fully charged, this will be equal to the present charge of the battery ($\min\{M_2, M_5\}$) plus the charge required to reach its maximum charge (Fig. 2ii). Since V^{3+} and V^{4+} are the reactants in charge operation, this latter term will be given by $\min\{M_3, M_4\}$.

Consequently, to be compatible with Eq. (10), the authors propose to define the overall battery SoC as:

$$\mathrm{SoC} = \frac{\min\{M_2, M_5\}}{\min\{M_2, M_5\} + \min\{M_3, M_4\}} \tag{14}$$

Note that, when the battery is balanced, (14) coincides with the classic expression (11).

3.2. State of health

The SoH is a figure of merit that compares the total capacity of a battery in the present condition (Q_M) with the ideal total capacity corresponding to a balanced system (Q_M^N), as expressed in Eq. (15). As in the previous subsection, the objective is to derive a mol-based expression for the SoH in terms of vanadium species that is compatible with the general definition (15), even in the presence of both types of electrolyte imbalance.

$$\mathrm{SoH} = \frac{Q_M}{Q_M^N} \tag{15}$$

In a balanced VRFB, the total number of moles in each side of the system will be the equal to $M_t/2$, being M_t the total number of vanadium moles in the system ($M_t = M_2 + M_3 + M_4 + M_5$). Furthermore, since the SoC at both sides will be also the same, all vanadium moles will be available to react in a balanced VRFB. Accordingly, its capacity will be given by $M_t/2 = M_2 + M_3 = M_4 + M_5$.

In contrast, the maximum charge that an imbalanced battery can deliver will be given by $\min\{M_2, M_5\} + \min\{M_3, M_4\}$, as discussed in Section 3.1. Therefore, the authors propose the following definition for the SoH in terms of the vanadium species number of moles:

$$\mathrm{SoH} = \frac{\min\{M_2, M_5\} + \min\{M_3, M_4\}}{M_t/2} \tag{16}$$

An illustrative example is presented in Fig. 3. The total number of moles in the system is 20, but, as a consequence of imbalance, these are not evenly distributed.

In the current state (Fig. 3i), applying Eq. (14) and (16) it is obtained that its corresponding SoC and SoH are 0.428 and 0.7, respectively. To better appreciate that the battery's capacity is a 70% of the original one, in the example, the battery is subsequently fully charged (Fig. 3ii), and then fully discharged (Fig. 3iii). Effectively, in such discharge, only 7 moles of reactant could be used for the reaction, in comparison to the 10 that would correspond to a balanced battery. It is worth mentioning that, as expected, the charge and discharge operations modify the battery's SoC, but do not affect its SoH. By comparing the three stages of Fig. 3, it can be easily checked that Eq. (16) gives always the same result independently of the SoC.

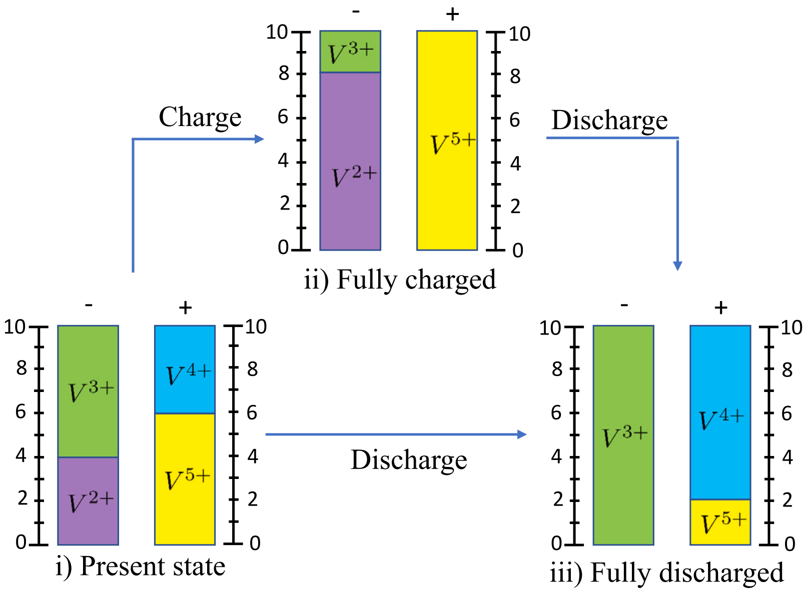

Fig. 2. Graphical demonstration of generalised SoC Eq. (14).

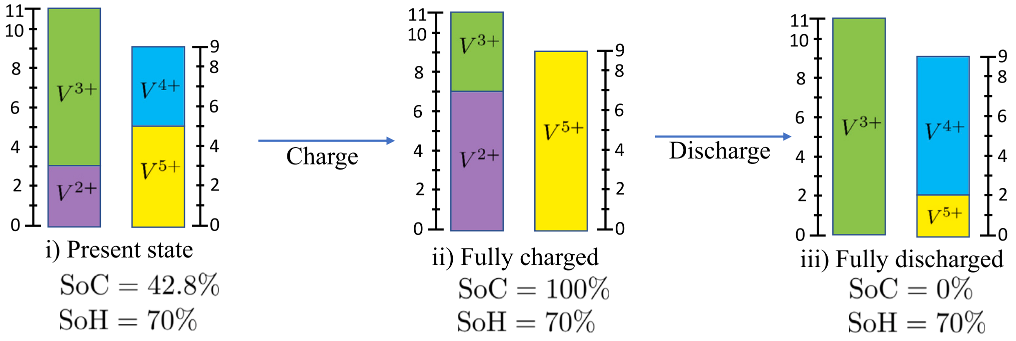

Fig. 3. Graphical demonstration of generalised SoH Eq. (16).

3.3. Retrievable state of health

As discussed in Section 2, the classic approach to restore the capacity of an imbalanced VRFB is electrolyte remix. Nonetheless, it has also been established that remixing is only effective to correct the capacity loss associated to stoichiometric imbalances. Therefore, in this section the authors define an indicator that allows to predict, beforehand, how effective the remix will be.

Before proceeding with the analysis, it is convenient to define the average oxidation state (AOS) of a VRFB as follows [36]:

$$\mathrm{AOS} = 2\frac{M_2}{M_t} + 3\frac{M_3}{M_t} + 4\frac{M_4}{M_t} + 5\frac{M_5}{M_t} \tag{17}$$

In a balanced VRFB, the AOS will be equal to +3.5. Nevertheless, when the battery suffers from faradaic imbalance, the AOS will shift to a higher value or, less likely, to a lower one. Note that, as reactions (3)–(6) do not involve electron transfer with species different from the vanadium ions, the AOS of a VRFB will not be modified in a remix operation. On the other hand, since species with non-adjacent oxidation states cannot coexist in the same container without reacting with each other [41], these reactions will proceed until V^{2+} and V^{5+} are completely exhausted. Hence, the final composition of a system after a remix operation can be obtained by applying the restrictions $M_{2,f} = 0$ and $M_{5,f} = 0$ and the conservation balances $M_{t,f} = M_{t,i}$ and $AOS_f = AOS_i$, with f indicating the final condition (after the remix) and i the initial condition (before the remix).

The effectiveness of the remix strategy can be graphically appreciated in Fig. 4. As in the previous examples, the whole system contains 20 vanadium moles. Fig. 4a depicts a VRFB that experiences stoichiometric imbalance which reduces its capacity in a 20% (SoH = 80%). After remixing, reactions (3)–(6) result in a solution of V^{3+} and V^{4+} in proportion 1:1, namely, $\mathrm{V}^{3.5+}$. Then, after charging, the battery would be perfectly balanced, effectively restoring it capacity up to SoH = 100%.

In contrast, in Fig. 4b, the battery suffers from oxidation that leads to faradaic imbalance. Specifically, the AOS rises from +3.5 to +3.6, reducing its SoH to 80%. After the remix, the resulting solution contains V^{3+} and V^{4+} in proportion 2:3, i.e., the AOS remains +3.6. Therefore, after charging operation, the imbalance is still present. In this case, the remix was completely ineffectual, and the SoH remains 80%.

In Fig. 4c, the battery undergoes both crossover and oxidation, resulting in a combination of stoichiometric and faradaic imbalance. This produce a loss of a 40% of the battery's capacity, resulting in a SoH = 60%. After the remix and charge operation, the stoichiometric imbalance is corrected, which entails a partial restoration of the capacity (SoH = 80%).

In Figs. 5b and 5c. it is possible to see that the only factor that affects the final capacity of the battery after the remix operation is the AOS. In this sense, it is possible to define the index Δq that quantifies the deviation of the AOS with respect to the value of +3.5 that corresponds to a balanced battery:

$$\Delta q = 2 \times (\mathrm{AOS} - 3.5) \tag{18}$$

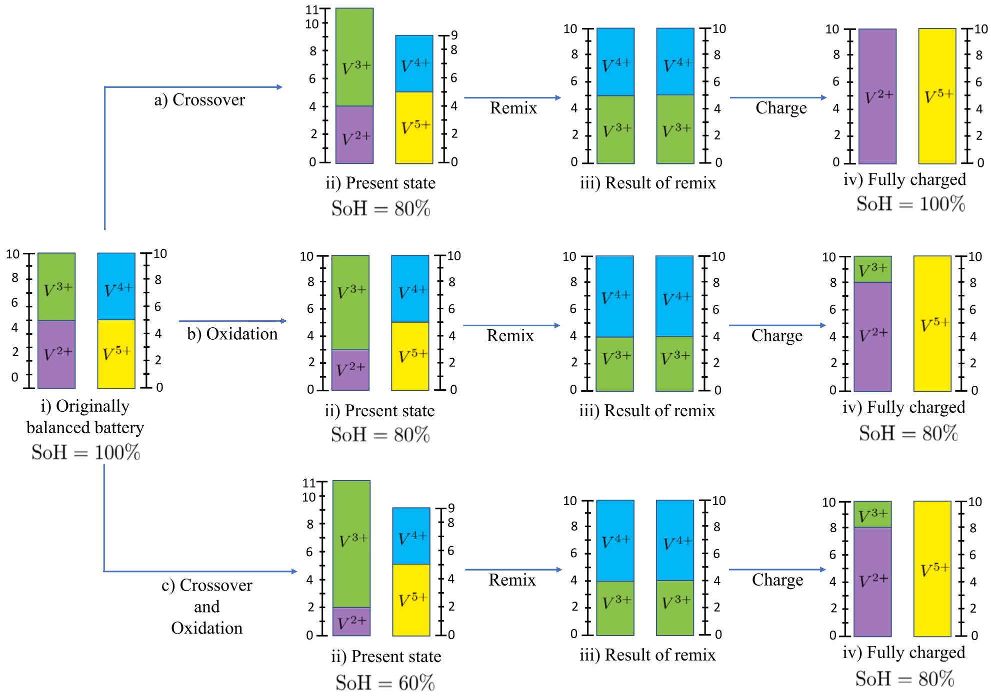

Fig. 4. Effect of electrolyte remix on a battery with: (a) stoichiometric imbalance; (b) faradaic imbalance; and (c) both stoichiometric and faradaic imbalance.

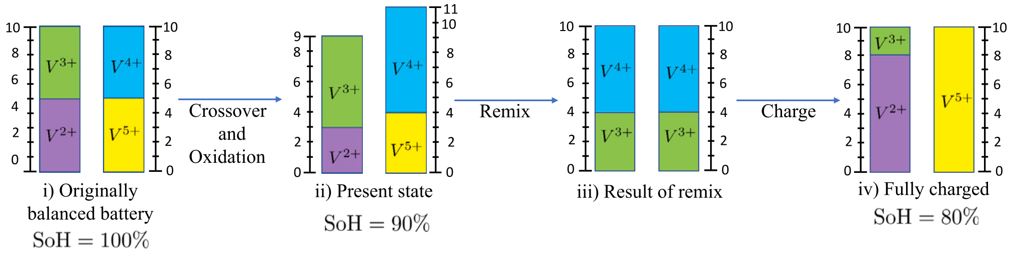

Fig. 5. Illustrative example of a counterproductive remix operation.

Given that the remix eliminates the stoichiometric imbalance, the SoH that the battery will have after this operation will be only a function of Δq. Consequently, the authors have defined a Retrievable State of Health (SoH_r), that permits to predict beforehand the SoH the battery would have if remixed:

$$\mathrm{SoH}_r = 1 - |\Delta q| \tag{19}$$

Note that, in certain cases, SoH_r may have a value that is actually lower than the present SoH. For instance, let us consider a VRFB that, at a certain moment contains the following number of moles: $[M_2;\ M_3;\ M_4;\ M_5] = [3;\ 6;\ 7;\ 4]$. Applying Eq. (16), it is obtained a SoH = 90%. In turn, (17) and (19) result in an AOS of +3.6 and a SoH_r of 80%. This result implies that the remix would actually reduce the battery's capacity instead of increasing it. Although this may seem counterintuitive, in Fig. 5 it can be clearly appreciated that, before the remix, the 9 vanadium moles contained in the negative electrolyte are available to participate in the charge/discharge operations. In contrast, after the remix, only 8 of them are available, as predicted.

In summary, by comparing SoH with SoH_r, it is possible to predict the efficiency of the remix strategy before conducting it. A $\mathrm{SoH}_r = 1$ implies a completely recovery of the battery's capacity, while a $\mathrm{SoH} < \mathrm{SoH}_r < 1$ means that only a partial recovery will be attained. Finally, it has been proved that the remix can also be counterproductive, which corresponds to a $\mathrm{SoH} > \mathrm{SoH}_r$.

4. Capacity loss mitigation

In this section, the effect of electrolyte imbalance over the battery's capacity is analysed. Special attention is drawn to the interaction between stoichiometric and faradaic imbalances. Based on this analysis, an strategy to mitigate the capacity fade originated by electrolyte imbalance is developed.

4.1. Relationship between electrolyte imbalance and capacity

Although Eq. (16) is very useful for calculating the battery's capacity, it does not allow to directly interpret the interaction between both types of imbalances. Furthermore, to decouple both sources of capacity loss is also advantageous for the development of control and optimisation strategies. Accordingly, it is convenient to rewrite Eq. (16) in terms of Δm and Δq, which represent each type of imbalance. Δq has been defined in the previous section, and allows to quantify the faradaic imbalance. Δm is defined in Eq. (20) to quantify the stoichiometric imbalance:

$$\Delta m = \frac{(M_4 + M_5) - (M_2 + M_3)}{M_t/2} \tag{20}$$

Specifically, Δm represents the difference between the vanadium moles in each side of the system, with respect to the number of moles each tank would have if the battery were balanced. Evidently, $\Delta m = 0$

Table 1
Classification of imbalance conditions in terms of remix effectiveness.

Case	Condition	Type of imbalance	Remix effect
1	$\Delta m = 0$; $\Delta q = 0$	Perfectly Balanced	No effect (maximum capacity)
2	$\Delta m \neq 0$; $\Delta q = 0$	Purely Stoichiometric	Fully restores capacity
3	$\Delta m = 0$; $\Delta q \neq 0$	Purely Faradaic	No effect
4	$\{\Delta m > 2\Delta q$ or $\Delta m < 0$; $\Delta q > 0\}$ or $\{\Delta m < 2\Delta q$ or $\Delta m > 0$; $\Delta q < 0\}$	Stoichiometric and Faradaic	Partially restores capacity
5	$\{0 < \Delta m < 2\Delta q$; $\Delta q > 0\}$ or $\{2\Delta q < \Delta m < 0$; $\Delta q < 0\}$	Stoichiometric and Faradaic	Negatively affects capacity

indicates that the battery is stoichiometrically balanced, while $\Delta m > 0$ and $\Delta m < 0$ corresponds to a net crossover towards the positive or negative side of the system, respectively.

The resulting expression for the SoH in terms of Δm and Δq is presented in Eqs. (21) and (22). The detailed demonstration of how (16) is transformed into (21) and (22) is provided in Appendix A.

Eq. (21) is valid for the region where the limiting reactant in discharge is V^{2+} (denoted as zone A), while (22) is valid for the complementary region (denoted as zone B), where the limiting reactant in discharge is V^{5+}. In turn, these regions can be subdivided into regions A.1 (Eq. (21a)), A.2 (Eq. (21b)), B.1(Eq. (22a)) and B.2 (Eq. (22b)) depending on the final expression of the SoH in terms of Δm and Δq.

For the Zone A ($\Delta m \leq 2\Delta q$):

$$\mathrm{SoH} = 1 - \min\{-\tfrac{\Delta m}{2}, \Delta m - \Delta q\} = \begin{cases} 1 - (\Delta q - \Delta m) & \text{if} \quad \Delta m \leq \dfrac{2}{3}\Delta q \quad (21a) \\ 1 - \dfrac{\Delta m}{2} & \text{if} \quad \Delta m > \dfrac{2}{3}\Delta q \quad (21b) \end{cases}$$

For the Zone B ($\Delta m > 2\Delta q$):

$$\mathrm{SoH} = 1 - \min\{\Delta m - \Delta q, \tfrac{\Delta m}{2}\} = \begin{cases} 1 - (\Delta m - \Delta q) & \text{if} \quad \Delta m \geq \dfrac{2}{3}\Delta q \quad (22a) \\ 1 + \dfrac{\Delta m}{2} & \text{if} \quad \Delta m < \dfrac{2}{3}\Delta q \quad (22b) \end{cases}$$

The SoH contour curves corresponding to (21) and (22) are plotted on the plane Δq-Δm represented in Fig. 6. Naturally, the maximum capacity (SoH = 1) corresponds with a $\Delta q = 0$ and $\Delta m = 0$ (i.e., a perfectly balanced VRFB), and decreases with the distance to this point.

Interestingly, the map presented in Fig. 6 is not symmetric with respect to the axes Δm and Δq. Hence, it can be appreciated that the capacity drops rapidly when the battery gets imbalanced towards the quadrants II ($\Delta q < 0$ and $\Delta m > 0$) and IV ($\Delta q > 0$ and $\Delta m < 0$) of the plane, while it decreases more slowly in the quadrants I ($\Delta q > 0$ and $\Delta m > 0$) and III ($\Delta q < 0$ and $\Delta m < 0$). In addition, it is possible to see that a certain change in Δq and Δm may have a different effect depending on the region where it occurs. For instance, in the quadrant I, an oxidative process (i.e., an increase in Δq) would have a negative impact on the SoH in zone A1, would be ineffective in zone A.2 and would be actually beneficial in zone B.1. Equivalently, a progressive imbalance towards positive Δm will have a greater adverse impact on capacity in zone B.1 than in zones A.1/A.2. The latter observation is precisely the theoretical basis of the experimental findings of [38], where it was shown that electrolytes with an AOS slightly higher than +3.5 exhibit a better capacity retention than with the ideal AOS=+3.5.

Fig. 6 also allows to interpret Eq. (19) in a graphical way. Specifically, the SoH_r will correspond to the SoH line that crosses the axis $\Delta m = 0$, without changing Δq. For instance, at the point $(\Delta q\ ,\ \Delta m) = (0.4\ ,\ 0.6)$, the SoH will be 0.7, and its SoH_r, corresponding to the point $(0.4\ ,\ 0)$, will be 0.6, this is, a case of counterproductive remix. Accordingly, the plane can be classified in terms of remix effectiveness, as shown in Fig. 7. The regions that make up that figure are formalised in Table 1.

4.2. Optimal remix strategy

In this subsection, the relationship between imbalance and capacity derived in the last subsection is used to develop an active strategy that outperforms standard remix. This allows to maximise the battery capacity in a simple way, mitigating the effects of faradaic imbalance and preventing the possibility of counterproductive remix.

In Fig. 6 it can be appreciated that, for every Δq, there will be an optimal Δm that maximises the battery's capacity. For instance, for a $\Delta q = 0.3$, the maximum capacity will be given by a SoH = 90% and corresponds to a Δm of 0.2. This capacity contrasts with the much lower SoH of 70% that the battery would have with the same faradaic imbalance ($\Delta q = 0.3$) but a null stoichiometric imbalance ($\Delta m = 0$). Specifically, the optimal Δm is located on the line $\Delta m = 2/3\Delta q$, that delimits zones A.1 and A.2, and B.1 and B.2, respectively. The formal proof of this observation is provided in Appendix B.

In the light of this finding, a strategy oriented to maximise the capacity of an imbalanced VRFB can be formulated. The objective will be to keep the system operating close to the maximum capacity line by periodically inducing optimal remixes. Hence, the negative effects of faradaic imbalance can be indirectly mitigated through the optimal regulation of Δm.

Accordingly, the steps of the proposed strategy are the following:

1. To determine the vanadium species concentration and volumes of the electrolytes. These values can be directly obtained by means of specific techniques [39], such as UV–vis spectroscopy or potentiometric titration. Moreover, estimators can be used to avoid the sensors but this particular topic is out of the scope of this paper.
2. To calculate the indexes Δm, using Eq. (20), and Δq, using Eq. (18), to quantify the stoichiometric and faradaic imbalances, respectively.
3. To determine the optimal Δm that minimises the capacity loss for the present Δq:

$$\Delta m^* = 2/3\Delta q \tag{23}$$

4. To calculate the necessary number of vanadium moles that need to be transferred from one electrolyte to the other in order to reach Δm^*. Starting from a battery that contains $M_n = M_2 + M_3$ and $M_p = M_4 + M_5$ moles at the negative and positive side, respectively:

$$\text{Before the remix:} \qquad \Delta m = \frac{M_p - M_n}{M_t/2} \tag{24}$$

$$\text{After the remix:} \qquad \Delta m^* = \frac{(M_p + M^*) - (M_n - M^*)}{M_t/2} \tag{25}$$

where M^* is the number of vanadium moles that need to be transferred from one tank to the other to maximise the capacity. A positive value of M^* indicates an electrolyte transfer from the negative tank to the positive one and vice versa. Then, M^* is obtained from (26):

$$M^* = \left(\frac{\Delta m^*\, M_t}{2} + M_n - M_p\right)/2 \tag{26}$$

5. To transfer an appropriate volume of electrolyte that contains M^*:

$$V^* = \begin{cases} \dfrac{|M^*|}{c_{v,n}} = \dfrac{|M^*|}{c_2 + c_3} & \text{if} \quad M^* > 0 \quad (27a) \\ \dfrac{|M^*|}{c_{v,p}} = \dfrac{|M^*|}{c_4 + c_5} & \text{if} \quad M^* < 0 \quad (27b) \end{cases}$$

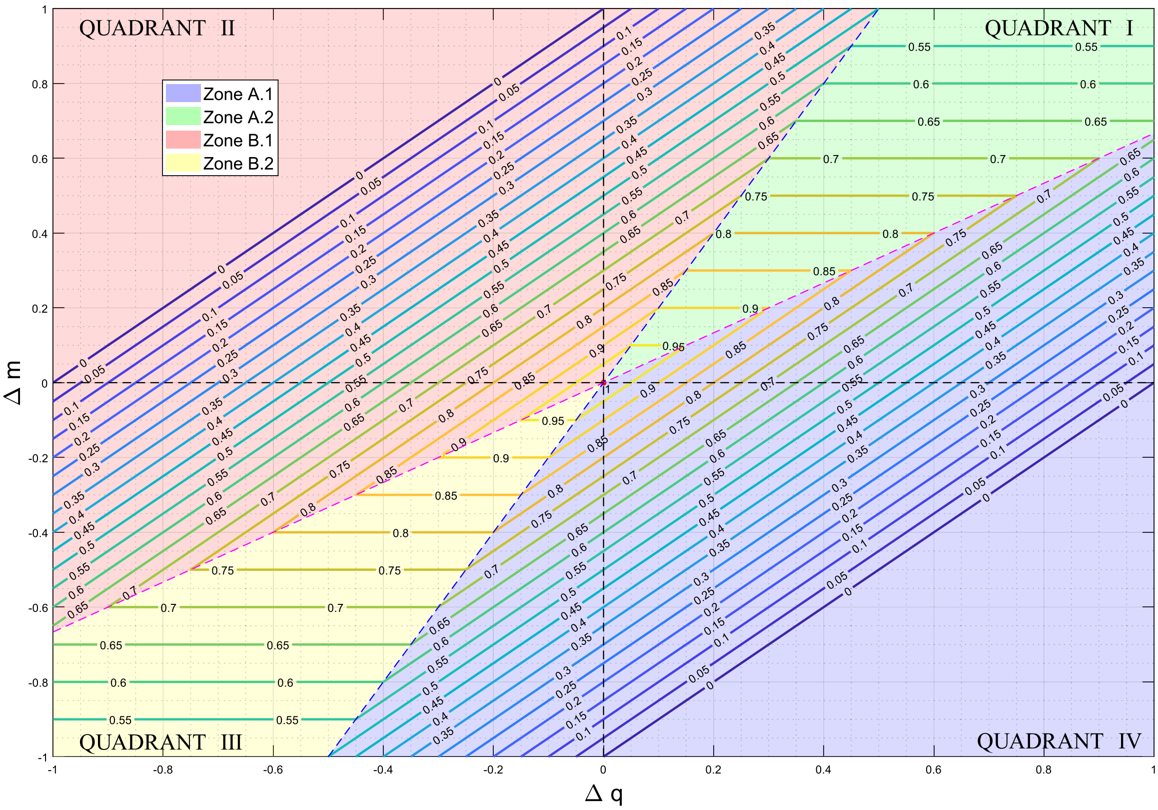

Fig. 6. SoH contour curves (capacity isolines) on the plane $\Delta q - \Delta m$. Each coloured region corresponds to a different zone of Eqs. (21) and (22).

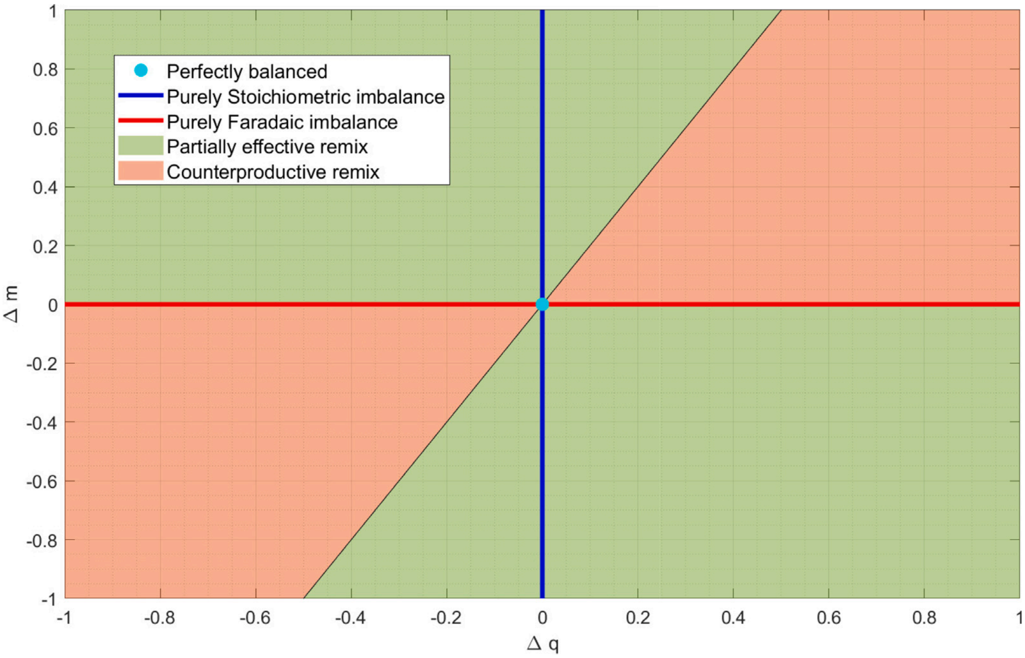

Fig. 7. Characterisation of the plane $\Delta q - \Delta m$ in terms of remix effectiveness.

where $c_{v,n}$ and $c_{v,p}$ is the total vanadium concentration in the negative and positive side of the system, respectively.

This strategy can be either conducted periodically, or when the battery reaches a minimum admissible capacity. In this way the capacity loss originated by faradaic imbalances, normally assumed to be completely irreversible, can be mitigated in a very simple and cost effective manner.

5. Results and discussion

In this section an illustrative example is presented to facilitate the comprehension and demonstrate the efficiency of the strategy proposed in Section 4.2. The behaviour of the VRFB is modelled through dynamic equations and simulated in MATLAB-Simulink. In Appendix C an additional example is provided to better clarify the comparison between

Table 2
VRFB sizing parameters.

Parameter	Meaning	Value	Units
c_v	Initial vanadium concentration	1.9	mol/l
d	Membrane thickness	$2 \cdot 10^{-4}$	m
E^0	Standard cell voltage	1.35	V
n	Number of cells	8	–
q	Electrolyte flow rate	1.6	l/min
Q_M^N	Initial capacity (balanced electrolytes)	40.2	A h
S	Membrane area	0.018	m^2
$V_{n,0}$	Initial anolyte volume	6.4	l
$V_{p,0}$	Initial catholyte volume	6.4	l

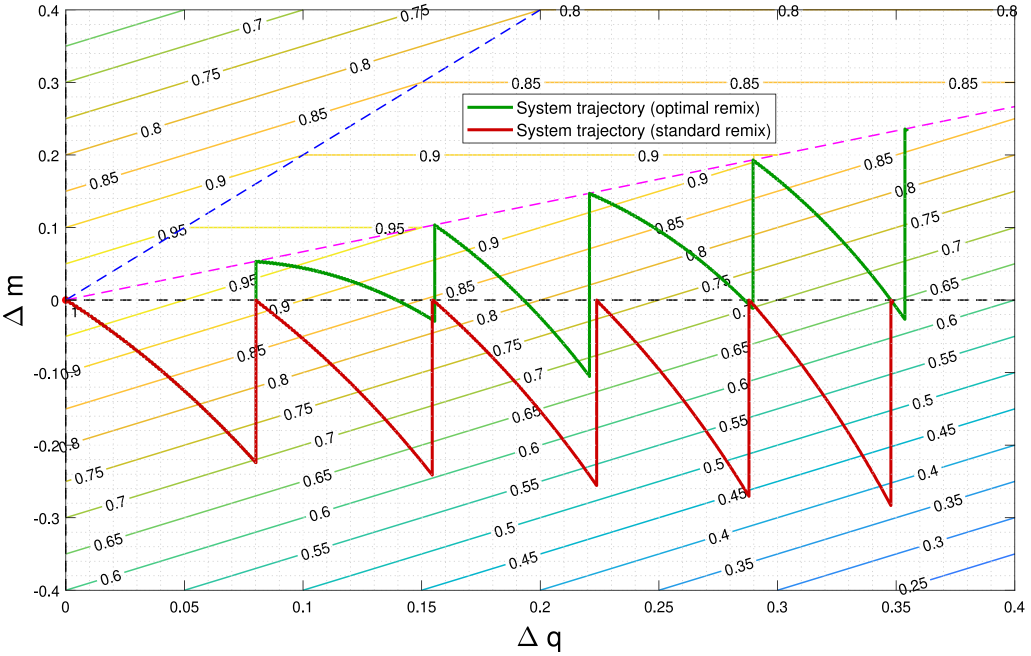

Fig. 8. System trajectory on the plane Δq-Δm, under a fixed-period remix schedule. Inclined segments correspond to a progressive imbalancing, while vertical jumps correspond to instantaneous remix operations.

the optimal and standard remixing strategies when Δm tends towards positive values.

In the example, the battery is subjected to 30 days of successive charge–discharge cycles, during which it undergoes different side reactions. In each cycle, the battery is charged until it reaches a SoC = 90% and then discharged until a SoC = 10%, being the current $I = \pm 15$ A. Despite starting from a perfectly balanced condition, these undesired phenomena gradually lead to stoichiometric and faradaic electrolyte imbalance. Then, in the simulations, the potential of the proposed methodology to deal with this imbalance and mitigate the capacity loss is assessed and contrasted to the standard remix approach.

The results have been obtained using a comprehensive eighth-order model that distinguishes between tank and cell concentrations. The model considers, in addition to the main electrochemical reactions, the phenomena of diffusion, convection and migration, as sources of stoichiometric imbalance; and of air oxidation and hydrogen evolution, as sources of faradaic imbalance. For the sake of space, the reader is referred to the work [5] where the complete model is presented, and the work [42] for the equations that describe the volume change dynamics originated by convection. The battery is sized as indicated in Table 2.

Over the course of the simulation, several remix operations are conducted to mitigate the capacity loss. Specifically, two different situations are considered. In the first case, presented in Fig. 8, the remix is performed in a fixed time interval of 6 days. In the second case, depicted in Fig. 9, the remix is triggered when the battery reaches a minimum acceptable capacity which, in this study, corresponds to a SoH = 60%.

Fig. 8 represents the trajectory of the system in a zoomed version of the plane $\Delta q - \Delta m$ presented in Fig. 6. It can be appreciated that the electrolytes tend to imbalance in the direction of negative Δm and positive Δq which results in an important decrease of the SoH. Every time a standard remix is performed, the value Δm is reset to 0, but Δq is not corrected, thus attaining only a limited recovery of the SoH. At the end of the considered period, after the fifth remix operation, the SoH is around 65%, which is a serious limitation to the VRFB performance in most practical applications.

In contrast, when the optimal remix operation is conducted, the value of Δm is taken to the line $\Delta m = 2/3\Delta q$. Therefore, although unable to fully restore the original capacity, the negative effects of electrolyte imbalance are substantially reduced. Specifically, at the end of the period, the SoH is around 88% which indicates that the battery's capacity is still remarkably high. In other words, the capacity loss with the optimal approach is only a 33% of the that of the standard approach, i.e., the loss is mitigated in a 67%. Therefore, the VRFB could be operated for a much longer time before having to conduct a chemical or electrochemical operation to fully rebalance the electrolytes.

It is important to remark that the latter result can be generalised. After conducting a standard remix, the resulting capacity will be SoH $= 1 - |\Delta q|$, as anticipated in Section 3.3. In contrast, in the optimal case, this will be SoH $= 1 - \frac{1}{3}|\Delta q|$, this is, a mitigation of two thirds of the capacity loss. The reader can easily verify this by evaluating Eqs. (21) and (22) in $\Delta m = 0$ and $\Delta m = 2/3\Delta q$, respectively.

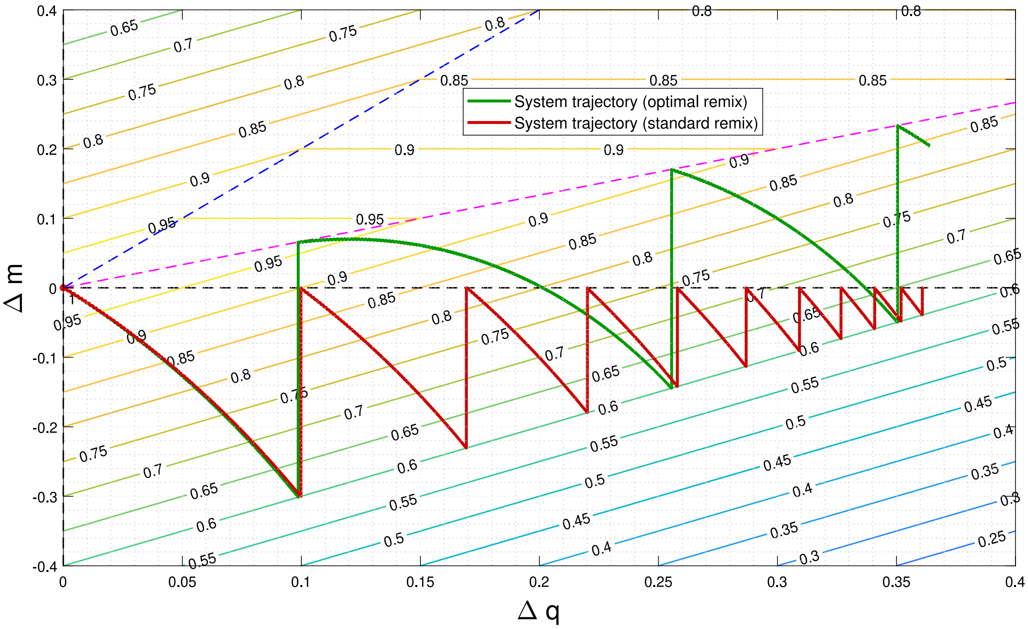

Fig. 9. System trajectory on the plane Δq-Δm, with a minimum capacity threshold corresponding to a SoH = 60%. Inclined segments correspond to a progressive imbalancing, while vertical jumps correspond to instantaneous remix operations.

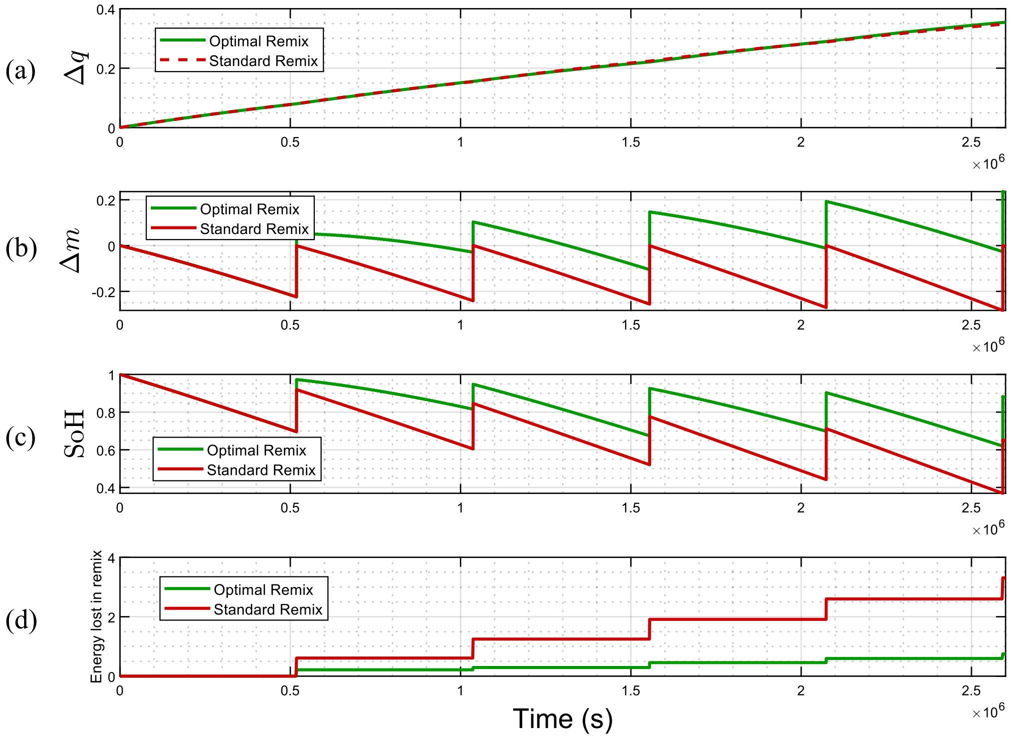

Fig. 10. Time evolution of the main variables, under the fixed-period remixing schedule. (a) Faradaic imbalance: Δq. (b) Stoichiometric imbalance: Δm. (c) State of Health: SoH. (d) Cumulative energy loss of remix operations, normalised with respect to the original battery capacity.

Fig. 9 considers the case in which the remix is not conducted periodically, but every time the capacity falls below a predefined minimum threshold. In this case, it is possible to see that the proposed strategy does not only result in a higher capacity, but also requires of less rebalancing operations. In particular, only 3 optimal remix operations are needed to keep the SoH above 60% in the considered period, in comparison to the 10 with the traditional approach. This is highly beneficial because it allows to run the battery for a longer time, avoiding unnecessary interruptions in its operation. Moreover, since the energy stored in the battery is lost every time a remix operation is conducted, the proposed approach also contributes to the minimisation of that loss.

With regard to the latter aspect it is important to highlight that, even in the fixed-period case of Fig. 8, the optimal remix is beneficial in terms of the energy loss. This is because standard remix involves a full mixing of the electrolytes, leading to an under-discharge state as presented in Fig. 4. Conversely, in the optimal remix operation, only a limited volume of electrolyte is transferred, reducing the impact

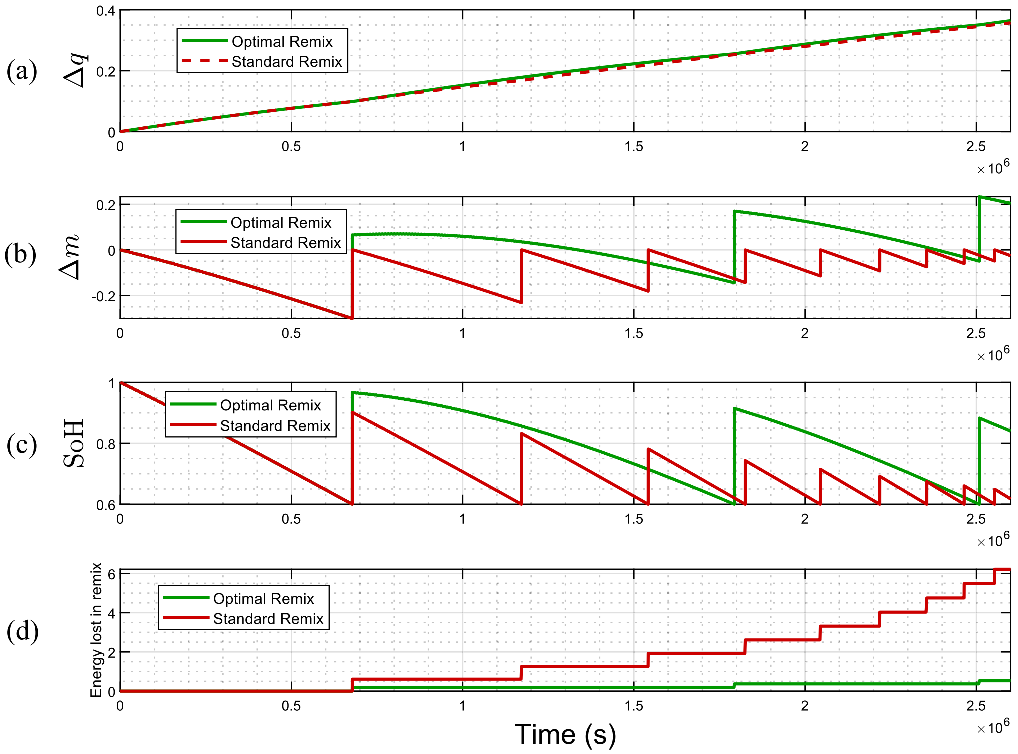

Fig. 11. Time evolution of the main variables, with a minimum capacity threshold of SoH = 60%. (a) Faradaic imbalance: Δq. (b) Stoichiometric imbalance: Δm. (c) State of Health: SoH. (d) Cumulative energy loss of remix operations, normalised with respect to the original battery capacity.

of the self discharge reactions (3)–(6). Accordingly, considering the parameters of the battery presented in Table 2 and a SoC = 10% at the moment of conducting the remix, the total charge loss in the fixed-period scenario will be equal to 133 Ah with a standard remix, and 31 Ah with the optimal one. In the minimum capacity scenario of Fig. 8, this difference is even more pronounced, being the charge loss equal to 280 Ah and 22 Ah with the standard and optimal remix, respectively.

Figs. 10 and 11 display the time evolution of the indexes Δq, Δm and SoH for the fixed-period and minimum-capacity remix cases, respectively. These complement the trajectories presented in Figs. 8 and 9 by explicitly including the time in the plots. Consequently, in these figures it is possible to see from a different perspective the effects of the rebalance operations. In accordance with the previous analysis, it is shown that every time a remix operation is conducted (either standard or optimal), the mass imbalance (Δm) experiences a sudden change in its value that, in turn, results in an improvement of the SoH. In contrast, the faradaic imbalance (Δq) remains unaffected, which explains the impossibility of achieving a full capacity recovery. Again, it is possible to see that in all the cases the capacity attained with the optimal operation, designed by taking into account the interaction between both types of imbalances, is much higher than with the standard remix.

Finally, in Figs. 10d and 11d, it is possible to graphically see the previously discussed benefits of the optimal strategy in terms of energy losses. That difference is accentuated during the second half of Fig. 11d, when the cumulative energy lost in remix operations increases sharply for the standard approach, while it remains low for the optimal one. To facilitate the comprehension of the plot, the cumulative energy loss is normalised with respect to the rated capacity of the battery, e.g. over the monthly simulation, the standard approach results in a total energy consumption equivalent to 6.2 times the battery's maximum charge.

6. Conclusion

In this paper, a comprehensive analysis of the effects of electrolyte imbalance on vanadium redox flow batteries' capacity has been developed. Specifically, it has been studied the interaction between stoichiometric imbalance, related to a difference in the number of vanadium moles at both sides of the system, and faradaic imbalance, originated by a net oxidation or reduction of the electrolytes. This study results not only in the deepening of the theoretical understanding of the battery behaviour but also in the development of a practical strategy with a direct impact on the system performance. The main specific outcomes are summarised as follows:

- Generalised State of Charge and State of Health indicators that consider both types of electrolyte imbalance have been formulated. With regard to the latter indicator, analytic expressions that explicitly decouple both sources of capacity loss have been derived.
- By resorting to the previous indicators, the effectiveness of the standard remix strategy on the battery capacity has been thoroughly assessed. This allows to systematically predict, beforehand, how effective the remix will be. Moreover, it has also been demonstrated that the remix may be counterproductive under certain imbalance conditions, further reducing the battery's State of Health instead of recovering it.
- It has been demonstrated that, for every value of faradaic imbalance there exists an optimal stoichiometric imbalance that maximises the battery capacity. By inducing optimal mass imbalances, the capacity loss could be mitigated up to a 67% in comparison with that resulting from a standard remix.
- Based on the previous point, a systematic strategy has been proposed to track that optimum in order to maximise the battery capacity recovery. Furthermore, that strategy also implies a reduction of the energy loss associated to the self discharge reactions that occur every time a remix is conducted. Finally, it is worth to remark that the proposed solution is of simple implementation and computationally low demanding.

The encouraging results obtained in this work pave the way for new research lines. Specifically, the authors are currently developing estimation methodologies to determine the vanadium species concentrations only from electric variable measures. Hence, the implementation of the

Table 3
Nomenclature and definitions.

Variable	Meaning	Unit
AOS	Average oxidation state of the VRFB	–
c_i	Concentration of V^{i+}	mol/l
I	Electric current	A
M_i	Moles of V^{i+}	mol
M_t	Total number of moles in the VRFB	mol
Δm	Stoichiometric (mass) imbalance index	–
Δq	Faradaic (oxidative/reductive) imbalance index	–
Q_M^N	Total capacity of the VRFB in an ideal balanced condition	A h
Q_M	Total capacity of the VRFB in the present condition	A h
Q	Electric charge currently stored in the VRFB	A h
SoC	State of Charge	–
SoH	State of Health	–
V	Electrolyte volume	l
Subscripts	**Meaning**	
$i \in \{2,3,4,5\}$	Oxidation state of the vanadium species	
n	Negative side of the system	
p	Positive side of the system	
$*$	Optimal imbalance line	

proposed optimal remix strategy will be straightforward in every VRFB system without need of any additional sensor. Furthermore, a techno-economical analysis that takes into account the specific application context is recommended to determine the best way to implement this strategy and dynamically optimise its frequency. Finally, the formal analysis of the effects of electrolyte imbalance will be utilised as a basis for the design of new control setups to further enhance VRFB's performance.

Nomenclature

See Table 3.

CRediT authorship contribution statement

Thomas Puleston: Conceptualization, Data curation, Formal analysis, Investigation, Methodology, Software, Visualization, Writing – original draft. **Maria Serra:** Funding acquisition, Project administration, Resources, Supervision, Validation, Visualization, Writing – review & editing. **Ramon Costa-Castelló:** Funding acquisition, Methodology, Project administration, Resources, Supervision, Writing – review & editing.

Declaration of competing interest

The authors declare that they have no known competing financial interests or personal relationships that could have appeared to influence the work reported in this paper.

Data availability

Data will be made available on request.

Acknowledgements

The project that gave rise to these results received the support of a fellowship from “la Caixa” Foundation (ID 100010434). The fellowship code is LCF/BQ/DI21/11860023. This work is part of the Project MAFALDA (PID2021-126001OB-C31) funded by MCIN/ AEI /10.13039/501100011033 and by “ERDF A way of making Europe”. This work is part of the project MASHED (TED2021-129927B-I00), funded by MCIN/ AEI/10.13039/50110 0011033 and by the European Union Next GenerationEU/PRTR.

Appendix A. Rearrangement of generalised SoH equation

The objective of this appendix is to show how (16) can be rearranged into Eqs. (21) and (22).

The present state of the battery is defined by the total number of moles of each vanadium species in the system: $\mathbf{x} = [M_2\ M_3\ M_4\ M_5]^\top$. The system can be transformed by defining the injective transformation $\Phi(\mathbf{x})$:

$$\Phi(\mathbf{x}) := \underbrace{\begin{bmatrix} M_t \\ \Delta M \\ \Delta Q \\ \text{SoC} \end{bmatrix}}_{\mathbf{z}} = \begin{bmatrix} M_2 + M_3 + M_4 + M_5 \\ M_4 + M_5 - M_2 - M_3 \\ -1.5M_2 - 0.5M_3 + 0.5M_4 + 1.5M_5 \\ \frac{\min\{M_2,M_5\}}{\min\{M_2,M_5\}+\min\{M_3,M_4\}} \end{bmatrix} \tag{A.1}$$

The analytic inverse of the transformation (A.1), $\Phi^{-1}(\mathbf{z})$, is rather lengthy given the nonlinearity of the SoC in terms of $\mathbf{x}$. Consequently, since $\Phi^{-1}(\mathbf{z})$ is not necessary to proceed with the demonstration, its expression is not included in this paper. In (A.1) M_t is the total moles of vanadium species in the system, while ΔQ and ΔM quantify the stoichiometric and faradaic imbalance of the battery, respectively.

By definition, the SoH is associated to the maximum charge the battery can provide, and thus, must not depend on the SoC, as demonstrated in Section 3.2. Therefore, the resulting expression for the SoH will be a function of M_t, ΔQ and ΔM but will be necessarily independent on the SoC. Accordingly, in order to conduct the demonstration, a SoC = 0 is arbitrarily assumed. It should be remarked (and the reader can easily check it) that any other value of SoC could be considered and the final result would remain the same.

A SoC = 0 means that either: (A) $M_2 = 0$, or (B) $M_5 = 0$.

In case (A), the transformation (A.1) gets reduced to the following equality:

$$\begin{bmatrix} M_t \\ \Delta M \\ \Delta Q \end{bmatrix} = \begin{bmatrix} 1 & 1 & 1 \\ -1 & 1 & 1 \\ -0.5 & 0.5 & 1.5 \end{bmatrix} \begin{bmatrix} M_3 \\ M_4 \\ M_5 \end{bmatrix} \tag{A.2}$$

And its inverse is:

$$\begin{bmatrix} M_3 \\ M_4 \\ M_5 \end{bmatrix} = \begin{bmatrix} 0.5 & -0.5 & 0 \\ 0.5 & 1 & -1 \\ 0 & -0.5 & 1 \end{bmatrix} \begin{bmatrix} M_t \\ \Delta M \\ \Delta Q \end{bmatrix} \tag{A.3}$$

In case (A), it holds that, when SoC = 0, $M_2 = 0$ and $M_5 \geq 0$. Therefore, the VRFB will be in case (A) when the following condition is fulfilled:

$$M_5 = -0.5\Delta M + \Delta Q \geq 0 \tag{A.4}$$

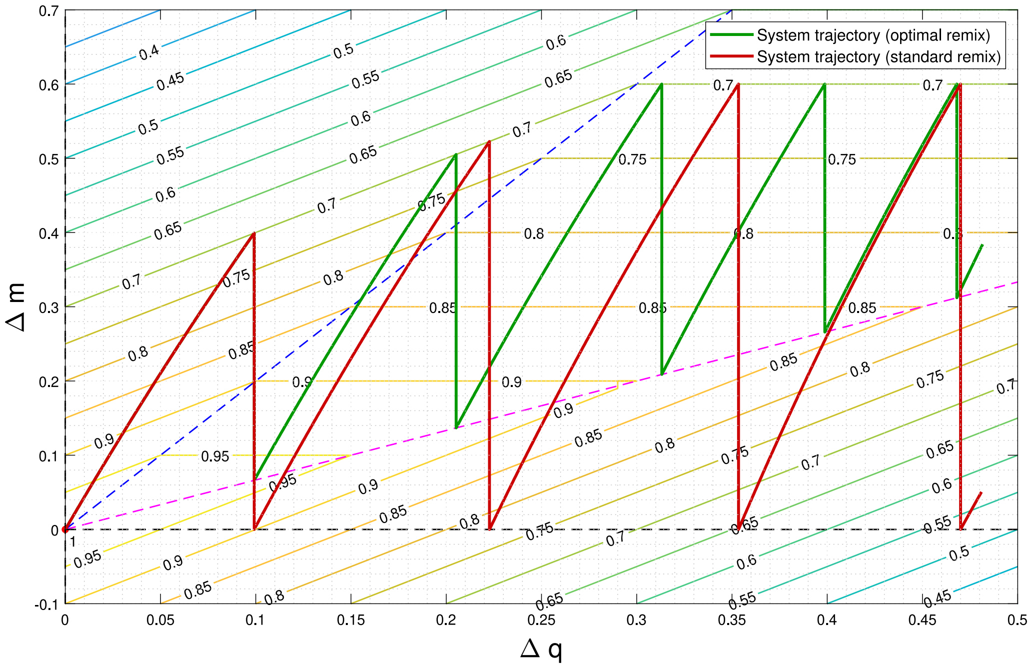

Fig. C.12. System trajectory on the plane Δq-Δm, with the imbalance occurring towards $\Delta m > 0$, and a minimum capacity threshold corresponding to a SoH = 70%.

Rearranging and dividing by $M_t/2$, this condition results:

$$\Delta m \leq 2\Delta q \tag{A.5}$$

Finally, the SoH for zone (A) in terms of the variables M_t, ΔM and ΔQ is obtained by substituting (A.3) in (16).

$$\mathrm{SoH} = \frac{\min\{0, -\Delta M/2 + \Delta Q\} + \min\{M_t/2 - \Delta M/2, M_t/2 + \Delta M - \Delta Q\}}{M_t/2} =$$

$$= \frac{M_t/2 + \min\{-\Delta M/2, \Delta M - \Delta Q\}}{M_t/2} = 1 + \min\{-\frac{\Delta m}{2}, \Delta m - \Delta q\} \tag{A.6}$$

which is precisely Eq. (21) that was to be demonstrated. Moreover, it is easy to see that the last term of (A.6) will be equal to $\frac{-\Delta m}{2}$ when $\Delta m \leq 2/3\Delta q$, and equal to $\Delta m - \Delta q$ when $\Delta m > 2/3\Delta q$.

The procedure to find the expression in case (B) is completely analogous to that for case (A). Here, Eq. (A.1) gets reduced to the following equality:

$$\begin{bmatrix} M_t \\ \Delta M \\ \Delta Q \end{bmatrix} = \begin{bmatrix} 1 & 1 & 1 \\ -1 & -1 & 1 \\ -1.5 & -0.5 & 0.5 \end{bmatrix} \begin{bmatrix} M_2 \\ M_3 \\ M_4 \end{bmatrix} \tag{A.7}$$

And its inverse is:

$$\begin{bmatrix} M_2 \\ M_3 \\ M_4 \end{bmatrix} = \begin{bmatrix} 0 & 1/2 & -1 \\ 1/2 & -1 & 1 \\ 1/2 & 1/2 & 0 \end{bmatrix} \begin{bmatrix} M_t \\ \Delta M \\ \Delta Q \end{bmatrix} \tag{A.8}$$

Now it holds that, when SoC = 0, $M_5 = 0$ and $M_2 > 0$. Therefore, the VRFB will be in case (B) when the following condition is fulfilled:

$$M_2 = 0.5\Delta M - \Delta Q > 0 \tag{A.9}$$

Rearranging and dividing by $M_t/2$, the condition results, as expected, in the complementary of the one for case (A):

$$\Delta m > 2\Delta q \tag{A.10}$$

Finally, the SoH for zone (B) in terms of the variables M_t, ΔM and ΔQ is obtained by substituting (A.8) in (16).

$$\mathrm{SoH} = \frac{\min\{\Delta M/2 - \Delta Q\ ,\ 0\} + \min\{M_t/2 - \Delta M + \Delta Q\ ,\ M_t/2 + \Delta M/2\}}{M_t/2} =$$

$$= \frac{M_t/2 + \min\{-\Delta M + \Delta Q\ ,\ \Delta M/2\}}{M_t/2} = 1 + \min\{-\Delta m + \Delta q\ ,\ \frac{\Delta m}{2}\} \tag{A.11}$$

which is precisely Eq. (22) that was to be demonstrated. Again, it is easy to see that the last term of (A.11) will be equal to $-\Delta m + \Delta q$ when $\Delta m \geq 2/3\Delta q$, and equal to $\frac{\Delta m}{2}$ when $\Delta m < 2/3\Delta q$.

Appendix B. Optimal mass imbalance proof

The objective is to demonstrate that, for every value of Δq, there exists a Δm that maximises the battery's capacity. Specifically, that maximum will be $\Delta m = 2/3\Delta q$.

For $\Delta q > 0$, the partial derivative with respect to Δm results:

$$\frac{\partial\, \mathrm{SoH}}{\partial\, \Delta m} = \begin{cases} 1 & \text{if} \quad \Delta m < 2/3\Delta q \quad \text{(Zone A.1)} \quad \text{(B.1a)} \\ -1/2 & \text{if} \quad 2/3\Delta q < \Delta m < 2\Delta q \quad \text{(Zone A.2)} \quad \text{(B.1b)} \\ -1 & \text{if} \quad \Delta m > 2\Delta q \quad \text{(Zone B.1)} \quad \text{(B.1c)} \end{cases}$$

The sign of Eq. (B.1) implies that the SoH is an increasing function with respect to Δm as long as $\Delta m < 2/3\Delta q$, and a decreasing function if $\Delta m > 2/3\Delta q$. Consequently, given that Eqs. (21) and (22) are continuous, the SoH will present a maximum at $\Delta m = 2/3\Delta q$.

Similarly, for $\Delta q < 0$, the partial derivative with respect to Δm results:

$$\frac{\partial\, \mathrm{SoH}}{\partial\, \Delta m} = \begin{cases} 1 & \text{if} \quad \Delta m < 2\Delta q \quad \text{(Zone A.1)} \quad \text{(B.2a)} \\ 1/2 & \text{if} \quad 2\Delta q < \Delta m < 2/3\Delta q \quad \text{(Zone B.2)} \quad \text{(B.2b)} \\ -1 & \text{if} \quad \Delta m > 2/3\Delta q \quad \text{(Zone B.1)} \quad \text{(B.2c)} \end{cases}$$

Again, the sign of Eq. (B.2) implies that the SoH is an increasing function with respect to Δm if $\Delta m < 2/3\Delta q$, and a decreasing function if $\Delta m > 2/3\Delta q$. Therefore, for every value of Δq the SoH will present a maximum at $\Delta m = 2/3\Delta q$.

Appendix C. Imbalancing towards positive Δm case study

The objective is to discuss some particular characteristics phenomena that take place when the imbalancing occurs towards Quadrant I of the plane $\Delta q - \Delta m$, which is a common situation for VRFBs employing cation exchange membranes. In this case, the simulations are based on the physicochemical parameters reported in [43], which result in a net crossover towards the positive side of the VRFB. The operating conditions of the simulation are the same as the ones presented in Section 5.

A minimum capacity threshold of SoH = 70% is considered to illustrate this case, as shown in Fig. C.12. It is firstly possible to note that, as discussed in Section 4.1, if $\Delta q > 0$, the capacity decay rate will be comparatively slower if crossover occurs towards the Quadrant I of the plane ($\Delta m > 0$) than to Quadrant IV ($\Delta m < 0$). Hence, in this case the system SoH does not reach values as low as those presented in Section 5.

In Fig. C.12 it is also possible to appreciate that, consistently with the previous examples, the capacity recovery attained with the optimal remix will always exceed that of the standard one. Furthermore, as anticipated in Section 4.1, it is in this case of an imbalance towards $\Delta m > 0$, that a counterproductive remixing operation may occur. Specifically, this happens in the third and fourth standard remixing operations, where the SoH drops from 70%, to 65% and 53%, respectively.

Finally, it should be noted that since the optimal remix always increases capacity, it guarantees that the SoH will be kept above the minimum admissible value. That is not the case of the standard one, that may lead the SoH to fall below that threshold, as it occurs in the third and fourth operations of this particular example. Therefore, although involving less re-balancing operations, the primary objective of keeping the SoH above 70% is not achieved in that case, portraying one of the main benefits of the optimal strategy.

References

[1] Yang Y, Bremner S, Menictas C, Kay M. Modelling and optimal energy management for battery energy storage systems in renewable energy systems: A review. Renew Sustain Energy Rev 2022;167. http://dx.doi.org/10.1016/j.rser.2022.112671.

[2] Frate GF, Ferrari L, Desideri U. Energy storage for grid-scale applications: Technology review and economic feasibility analysis. Renew Energy 2021;163:1754–72. http://dx.doi.org/10.1016/j.renene.2020.10.070.

[3] Bogdanov S, Pugach M, Parsegov S, Vlasov V, Ibanez FM, Stevenson KJ, et al. Dynamic modeling of vanadium redox flow batteries: Practical approaches, their applications and limitations. J Energy Storage 2023;57:106191. http://dx.doi.org/10.1016/j.est.2022.106191.

[4] Sánchez-Díez E, Ventosa E, Guarnieri M, Trovò A, Flox C, Marcilla R, et al. Redox flow batteries: Status and perspective towards sustainable stationary energy storage. J Power Sources 2021;481. http://dx.doi.org/10.1016/j.jpowsour.2020.228804.

[5] Puleston T, Clemente A, Costa-Castelló R, Serra M. Modelling and estimation of vanadium redox flow batteries: A review. Batteries 2022;8. http://dx.doi.org/10.3390/batteries8090121.

[6] Poli N, Trovò A, Fischer P, Noack J, Guarnieri M. Electrochemical rebalancing process for vanadium flow batteries: Sizing and economic assessment. J Energy Storage 2023;58. http://dx.doi.org/10.1016/j.est.2022.106404.

[7] Jirabovornwisut T, Arpornwichanop A. A review on the electrolyte imbalance in vanadium redox flow batteries. Int J Hydrogen Energy 2019;44:24485–509. http://dx.doi.org/10.1016/j.ijhydene.2019.07.106.

[8] Rodby KE, Carney TJ, Gandomi YA, Barton JL, Darling RM, Brushett FR. Assessing the levelized cost of vanadium redox flow batteries with capacity fade and rebalancing. J Power Sources 2020;460. http://dx.doi.org/10.1016/j.jpowsour.2020.227958.

[9] Lourenssen K, Williams J, Ahmadpour F, Clemmer R, Tasnim S. Vanadium redox flow batteries: A comprehensive review. J Energy Storage 2019;25:100844. http://dx.doi.org/10.1016/j.est.2019.100844.

[10] Nourani M, Dennison CR, Jin X, Liu F, Agar E. Elucidating effects of faradaic imbalance on vanadium redox flow battery performance: Experimental characterization. J Electrochem Soc 2019;166:A3844–51. http://dx.doi.org/10.1149/2.0851915jes.

[11] Satola B, Komsiyska L, Wittstock G. Corrosion of graphite-polypropylene current collectors during overcharging in negative and positive vanadium redox flow battery half-cell electrolytes. J Electrochem Soc 2018;165(5):A963. http://dx.doi.org/10.1149/2.0921805jes.

[12] Zhang Y, Liu L, Xi J, Wu Z, Qiu X. The benefits and limitations of electrolyte mixing in vanadium flow batteries. Appl Energy 2017;204:373–81. http://dx.doi.org/10.1016/j.apenergy.2017.07.049.

[13] Skyllas-Kazacos M, Kazacos M. State of charge monitoring methods for vanadium redox flow battery control. J Power Sources 2011;196:8822–7. http://dx.doi.org/10.1016/j.jpowsour.2011.06.080.

[14] Poli N, Schäffer M, Trovò A, Noack J, Guarnieri M, Fischer P. Novel electrolyte rebalancing method for vanadium redox flow batteries. Chem Eng J 2021;405. http://dx.doi.org/10.1016/j.cej.2020.126583.

[15] Skyllas-Kazacos M, Goh L. Modeling of vanadium ion diffusion across the ion exchange membrane in the vanadium redox battery. J Membr Sci 2012;399–400:43–8. http://dx.doi.org/10.1016/j.memsci.2012.01.024.

[16] Guarnieri M, Mattavelli P, Petrone G, Spagnuolo G. Vanadium redox flow batteries: Potentials and challenges of an emerging storage technology. IEEE Ind Electron Mag 2016;10:20–31. http://dx.doi.org/10.1109/MIE.2016.2611760.

[17] Esan O, Shi X, Pan Z, Huo X, An L, Zhao T. Modeling and simulation of flow batteries. Adv Energy Mater 2020;10. http://dx.doi.org/10.1002/aenm.202000758.

[18] Fornaro P, Puleston T, Puleston P, Serra-Prat M, Costa-Castelló R, Battaiotto P. Redox flow battery time-varying parameter estimation based on high-order sliding mode differentiators. Int J Energy Res 2022. http://dx.doi.org/10.1002/er.8319.

[19] Tang A, Bao J, Skyllas-Kazacos M. Dynamic modelling of the effects of ion diffusion and side reactions on the capacity loss for vanadium redox flow battery. J Power Sources 2011;196:10737–47. http://dx.doi.org/10.1016/j.jpowsour.2011.09.003.

[20] Pugach M, Kondratenko M, Briola S, Bischi A. Zero dimensional dynamic model of vanadium redox flow battery cell incorporating all modes of vanadium ions crossover. Appl Energy 2018;226:560–9. http://dx.doi.org/10.1016/j.apenergy.2018.05.124.

[21] Li Z, Liu L, Zhao Y, Xi J, Wu Z, Qiu X. The indefinite cycle life via a method of mixing and online electrolysis for vanadium redox flow batteries. J Power Sources 2019;438. http://dx.doi.org/10.1016/j.jpowsour.2019.226990.

[22] Schweiss R, Pritzl A, Meiser C. Parasitic hydrogen evolution at different carbon fiber electrodes in vanadium redox flow batteries. J Electrochem Soc 2016;163:A2089–94. http://dx.doi.org/10.1149/2.1281609jes.

[23] Shah AA, Al-Fetlawi H, Walsh FC. Dynamic modelling of hydrogen evolution effects in the all-vanadium redox flow battery. Electrochim Acta 2010;55:1125–39. http://dx.doi.org/10.1016/j.electacta.2009.10.022.

[24] Sun CN, Delnick FM, Baggetto L, Veith GM, Zawodzinski TA. Hydrogen evolution at the negative electrode of the all-vanadium redox flow batteries. J Power Sources 2014;248:560–4. http://dx.doi.org/10.1016/j.jpowsour.2013.09.125.

[25] Al-Fetlawi H, Shah AA, Walsh FC. Modelling the effects of oxygen evolution in the all-vanadium redox flow battery. Electrochim Acta 2010;55:3192–205. http://dx.doi.org/10.1016/j.electacta.2009.12.085.

[26] Choi NH, kwan Kwon S, Kim H. Analysis of the oxidation of the V(II) by dissolved oxygen using UV-visible spectrophotometry in a vanadium redox flow battery. J Electrochem Soc 2013;160:A973–9. http://dx.doi.org/10.1149/2.145306jes.

[27] Ngamsai K, Arpornwichanop A. Investigating the air oxidation of V(II) ions in a vanadium redox flow battery. J Power Sources 2015;295:292–8. http://dx.doi.org/10.1016/j.jpowsour.2015.06.157.

[28] Schofield K, Musilek P. State of charge and capacity tracking in vanadium redox flow battery systems. Clean Technol 2022;4(3):607–18. http://dx.doi.org/10.3390/cleantechnol4030037.

[29] Wang K, Liu L, Xi J, Wu Z, Qiu X. Reduction of capacity decay in vanadium flow batteries by an electrolyte-reflow method. J Power Sources 2017;338:17–25. http://dx.doi.org/10.1016/j.jpowsour.2016.11.031.

[30] Schafner K, Becker M, Turek T. Capacity balancing for vanadium redox flow batteries through continuous and dynamic electrolyte overflow. J Appl Electrochem 2021;51:1217–28. http://dx.doi.org/10.1007/s10800-021-01572-y.

[31] Bhattarai A, Wai N, Schweiss R, Whitehead A, Scherer GG, Ghimire PC, et al. Vanadium redox flow battery with slotted porous electrodes and automatic rebalancing demonstrated on a 1 kW system level. Appl Energy 2019;236:437–43. http://dx.doi.org/10.1016/j.apenergy.2018.12.001.

[32] Lu M, Yang W, Deng Y, Xu Q. An optimal electrolyte addition strategy for improving performance of a vanadium redox flow battery. Int J Energy Res 2020;44:2604–16. http://dx.doi.org/10.1002/er.4988.

[33] Mu D, Zhao Y, Yu L, Liu L, Xi J. Asymmetric vanadium flow batteries: Long lifespan via an anolyte overhang strategy. Phys Chem Chem Phys 2017;19:29195–203. http://dx.doi.org/10.1039/c7cp06249d.

[34] Shin J, Kim C, Jeong B, Vaz N, Ju H. New operating strategy for all-vanadium redox flow batteries to mitigate electrolyte imbalance. J Power Sources 2022;526. http://dx.doi.org/10.1016/j.jpowsour.2022.231144.

[35] Lu MY, Yang WW, Deng YM, Li WZ, Xu Q, He YL. Mitigating capacity decay and improving charge-discharge performance of a vanadium redox flow battery with asymmetric operating conditions. Electrochim Acta 2019;309:283–99. http://dx.doi.org/10.1016/j.electacta.2019.04.032.

[36] Loktionov P, Konev D, Pichugov R, Petrov M, Antipov A. Calibration-free coulometric sensors for operando electrolytes imbalance monitoring of vanadium redox flow battery. J Power Sources 2023;553. http://dx.doi.org/10.1016/j.jpowsour.2022.232242.

[37] Roznyatovskaya N, Herr T, Küttinger M, Fühl M, Noack J, Pinkwart K, et al. Detection of capacity imbalance in vanadium electrolyte and its electrochemical regeneration for all-vanadium redox-flow batteries. J Power Sources 2016;302:79–83. http://dx.doi.org/10.1016/j.jpowsour.2015.10.021.

[38] Wang Z, Guo Z, Ren J, Li Y, Liu B, Fan X, et al. An electrolyte with elevated average valence for suppressing the capacity decay of vanadium redox flow batteries. ACS Cent Sci 2022. http://dx.doi.org/10.1021/acscentsci.2c01112.

[39] Nolte O, Volodin IA, Stolze C, Hager MD, Schubert US. Trust is good, control is better: A review on monitoring and characterization techniques for flow battery electrolytes. Mater Horiz 2021;8:1866–925. http://dx.doi.org/10.1039/d0mh01632b.

[40] Clemente A, Cecilia A, Costa-Castelló R. Online state of charge estimation for a vanadium redox flow battery with unequal flow rates. J Energy Storage 2023;60:106503. http://dx.doi.org/10.1016/j.est.2022.106503.

[41] Sun J, Shi D, Zhong H, Li X, Zhang H. Investigations on the self-discharge process in vanadium flow battery. J Power Sources 2015;294:562–8. http://dx.doi.org/10.1016/j.jpowsour.2015.06.123.

[42] Song Y, Li X, Xiong J, Yang L, Pan G, Yan C, et al. Electrolyte transfer mechanism and optimization strategy for vanadium flow batteries adopting a Nafion membrane. J Power Sources 2020;449. http://dx.doi.org/10.1016/j.jpowsour.2019.227503.

[43] Yang XG, Ye Q, Cheng P, Zhao TS. Effects of the electric field on ion crossover in vanadium redox flow batteries. Appl Energy 2015;145:306–19. http://dx.doi.org/10.1016/j.apenergy.2015.02.038.